TEMPERATURE DISTRIBUTION IN DIODE-END-PUMPED LiF:F_2^- LASER CRYSTALS

Manuel Lopes Fº, Niklaus U. Wetter, Edison P. Maldonado
Divisão de Materiais Optoeletrônicos, IPEN/CNEN-SP, CP.11049, CEP 05422-970
E-mail: mlopes@net.ipen.br

The steady state thermal profiles due to CW, longitudinally diode laser pumping in LiF:F_2^- laser crystals were obtained by solving the thermal diffusion equation using Fourier series expansion. The longitudinally exponential drop of the pumping beam power was also considered, in the case of non-saturated optical absorption. Using this model, some designs that posses different conditions of pumping and cooling were simulated, allowing the estimates of the absolute values as well as the gradient of temperature inside the laser medium.

Introduction

It is well known that the longitudinal diode laser pumping of laser crystals leads to high optical efficiencies, typically of the order of 60%. However, significant part of the energy is dissipated as phonons, causing a non-homogeneous heating of the laser medium, with magnitude proportional to the host thermal conductivity and the constraints condition. This thermal distribution leads to gradients of refraction index, depending also on the material elasto-optic coefficients, that cause optical effects like induced lens, birefringence and aberrations [2,3]. There is also a maximum pumping power given by the breakdown limit of the laser crystal due to the increase of induced stress [2].

In order to develop high power lasers, it is imperative to calculate the induced thermal effects. Generally, the temperature and stress distributions can be determined by numerical approaches. In this work, we show analytic expressions for the temperature distribution in longitudinally pumped laser crystals for different pumping and cooling conditions. We have used basically the method presented in reference [1], which analyzed the case of transversal pumping for different geometries.

Theory

The considered pumping beam has rectangular shape, with sides δ_x e δ_y, propagating in the z direction. The beam is incident in a block of LiF:F_2^- crystal with length h_z and sides h_x and h_y. The dimension h_z is considered short, such that the beam profile is approximately constant over the laser medium. The beam intensity inside the laser medium is given by equation (1), where κ is the optical absorption coefficient.

$$I(x,y,z) = \frac{Po}{\delta_x \cdot \delta_y} \cdot e^{-\kappa\left(z+\frac{h_z}{2}\right)} \quad (1)$$

The thermal distribution is obtained by solving the diffusion equation $K.\nabla^2 T = Q$, where K is the thermal conductivity, T is the temperature and Q is the density of energy converted in heat that is given by $Q = -\eta.(\partial/\partial z)I(x,y,z)$, where η is the thermal conversion efficiency.

The considered active medium has ideal cooling at faces $x=\pm h_x/2$, where the constant temperature is in equilibrium with the cooling fluid. The remaining faces are in contact with air, have smaller areas, being therefore considered isolated. Thus, the boundary conditions are (2).

(2) $T = T_0$ for $x=\pm h_x/2$; $\frac{\partial T}{\partial z} = 0$ for $z=\pm h_z/2$; $\frac{\partial T}{\partial y} = 0$ for $y=\pm h_y/2$

The diffusion equation is solved by using two-dimensional Fourier series expansions in x and y. The obtained solution must satisfy the diffusion equation as well as the boundary conditions. Due to the heating source as well the boundary conditions have the symmetry planes x = 0 e y = 0, the Fourier terms are reduced to cosine functions and one obtains the equation (3).

(3)
$$T(x,y,z)=\sum_m\sum_n\left[\left(A_{m,n}\cdot e^{\gamma_{m,n}\cdot z}+B_{m,n}\cdot e^{-\gamma_{m,n}\cdot z}-\frac{e^{-\kappa\cdot\left(z+\frac{h_z}{2}\right)}\cdot u_{m,n}}{K\cdot\left(\kappa^2-\gamma^2_{m,n}\right)}\right)\cdot\cos(\beta_m\cdot y)\cdot\cos(\alpha_n\cdot x)\right]$$

where:

$$A_{m,n}=\frac{\kappa^2\cdot u_{m,n}\cdot e^{-\gamma_{m,n}\cdot\frac{h_z}{2}}\cdot\left(e^{-\gamma_{m,n}\cdot\frac{h_z}{2}}-e^{-\kappa\cdot h_z}\right)}{K\cdot\gamma_{m,n}\cdot\left(\kappa^2-\gamma^2_{m,n}\right)\cdot\left(1-e^{-2\cdot\gamma_{m,n}\cdot h_z}\right)} \qquad B_{m,n}=\frac{\kappa^2\cdot u_{m,n}\cdot e^{-\gamma_{m,n}\cdot\frac{h_z}{2}}\cdot\left(1-e^{-(\kappa+\gamma_{m,n})h_z}\right)}{K\cdot\gamma_{m,n}\cdot\left(\kappa^2-\gamma^2_{m,n}\right)\cdot\left(1-e^{-2\cdot\gamma_{m,n}\cdot h_z}\right)}$$

$$\alpha_n=\frac{2\cdot n+1}{h_x}\pi \qquad \beta_m=\frac{2\cdot m}{h_y}\pi \qquad \gamma_{m,n}=\left(\alpha^2{}_n+\beta^2{}_m\right)^{\frac{1}{2}}$$

$$u_{m,n}=\frac{4\cdot Q}{U_{m,n}\cdot}\cdot\operatorname{sen}\left(\frac{\delta_y\cdot\beta_m}{2}\right)\cdot\operatorname{sen}\left(\frac{\delta_x\cdot\alpha_m}{2}\right)$$

$$U_{m,n}=\frac{h_x\cdot h_y}{2}\ \text{se } m=0 \qquad U_{m,n}=\frac{h_x\cdot h_y}{4}\ \text{se } m\neq 0$$

Graphic simulations

We have considered the diode laser beam power as P_o = 10 W, incident on the LiF:F_2^- crystal at the face z = - $h_z/2$. The other considered parameters for the LiF:F_2^- crystal were: thermal conversion efficiency η = 0.4 [4], thermal conductivity K = 11.3 W/mK and optical absorption coefficient κ = 150 m^{-1} [5]. We analyzed three cases with different sizes and orientation of both the laser crystal and pumping beam. We have also considered the smallest transversal dimensions possible δ_x e δ_y for the pumping beam at its focal plane, which are limited by the beam quality from high power diode arrays. For typical diode arrays beam quality $M_i^2 \cong 1700$ and $M_j^2 \cong 1.4$, one have $\delta_i \cong 1.8$mm and $\delta_j \cong 0.16$mm. The M^2 values can be also distributed between the orthogonal directions, by using beam-shaping techniques, leading to symmetric beam profiles.

Figure (1a), (1b) and (2a) represent the temperature variation in LiF:F_2^- crystals at the entrance plane. In case (1a) and (1b), it were considered the same crystal dimensions and relative orientations of the (asymmetric) pumping beam, but cooling at different faces. In the case shown in figure (2a) it was considered symmetric pumping beam and crystal cross-section dimensions.

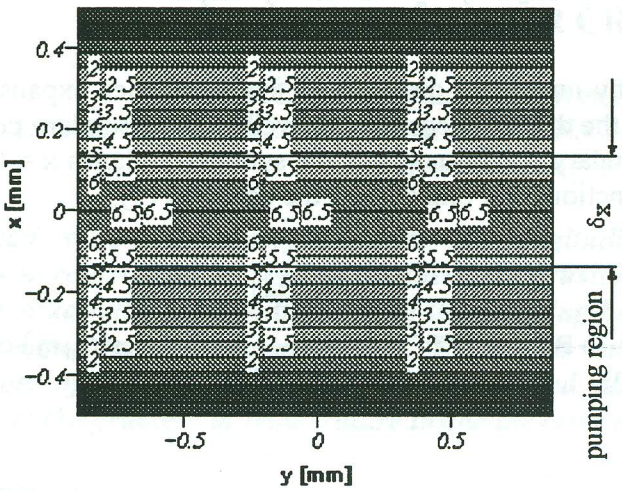

Figure (1a)

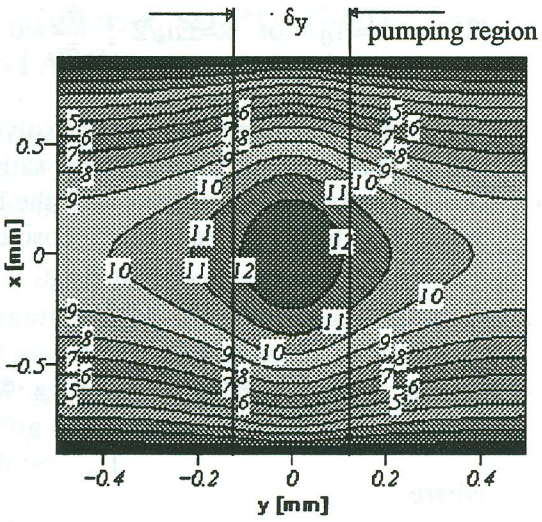

Figure (1b)

Figure (1a): Temperature variation [°C] at the pumping face, $z = -h_z/2$. The crystal dimensions are $h_y = 1.8$ mm, $h_x = 1.0$ mm and $h_z = 12$ mm. The pump beam dimensions are $\delta_x = 0.16$ mm and $\delta_y = 1.8$ mm. The boundary conditions are given by (2).

Figure (1b): Temperature variation [°C] at the pumping face, $z = -h_z/2$. The crystal dimensions and pumping beam relative orientation are identical to the case (1a), but with boundary conditions rotated.

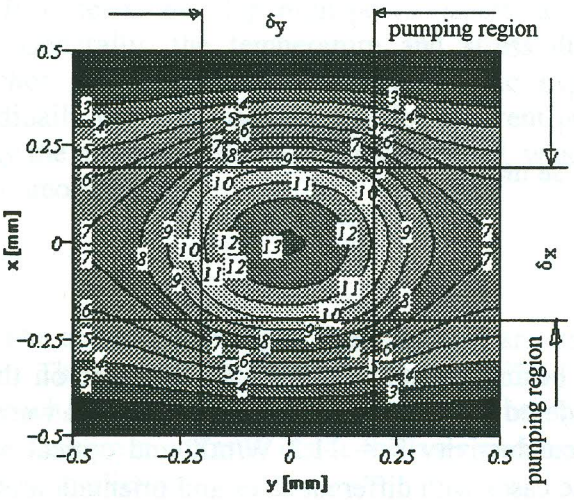

Figure (2a)

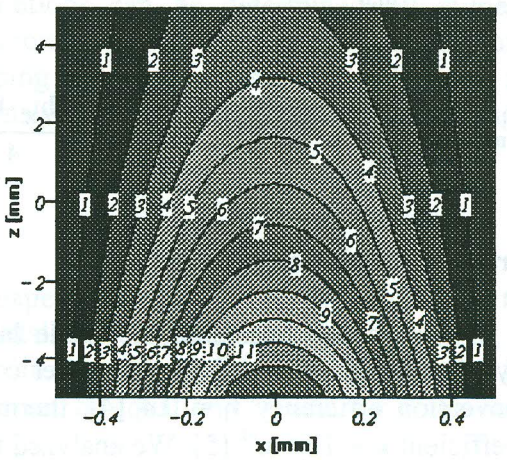

Figure (2b)

Figure(2a): Temperature variation [°C] at the pumping face, $z = -h_z/2$. The crystal dimensions are $h_y = 1.0$ mm, $h_x = 1.0$ mm and $h_z = 10$ mm. The pump beam dimensions are $\delta_x = 0.44$ mm and $\delta_y = 0.44$ mm. The boundary conditions are given by (2).

Figure (2b): Temperature variation [°C] at the plane y=0. The crystal and pumping beam dimensions are identical to those in (2a).

Conclusion

The minimum thermal gradient inside the active medium was obtained for the geometry considered in Figure (1a), with a temperature increase of only 6.5°C at the center of the crystal pumping face. However, as the temperature profile follow a rectangular geometry (and thus the refraction index modulation), only a poor coupling with circular-shaped intracavity mode is possible. In this case, laser modes with elliptical shape are more suitable in order to minimize optical distortions at the gain region (that consist in losses) and provide high values of gain. This requires a resonator using cylindrical mirrors, thus leading to a higher level of sophistication in the optical set-up.

The geometry considered in Figure (1b) has leaded to a temperature gradient two times higher, but the pumped region has, at its center, a temperature profile with circular symmetry. This condition allows coupling with a circular-shaped intracavity mode, with minor distortions, but using only part of the total pumped volume.

The coupling with circular-shaped intracavity modes can be further enhanced if high power diode lasers with beam quality factors $M^2_i > 1700$ were available, or if beam-shapers were used. The latter was studied in Figure (2a), where the symmetric profile of the pumping beam leads to a temperature distribution approximately circular over almost all the pumped region, in spite of the rectangular boundary conditions.

The thermal distribution obtained by this procedure, T(x,y,z), allows the calculation of this induced (thick) lens as an intracavity element. The longitudinal dependence of the temperature profile, in the case considered in Figure (2a), is shown in Figure(2b).

For the longitudinally pumped LiF:F_2^- laser, it is also essential minimize the temperature rise in any site of the gain region, due to the known thermal instability of the F_2^- color-centers, destroyed by temperature-favored migration processes.

References

[1] Pratrice Hello, Eric Durand et al, Thermal effects in Nd:YAG slabs 3D modeling and comparison with experiments, Journal of Modern Optics, pp. 1371-1390, vol. 41 #7, 1994.

[2] W. Koechner, Solid State Laser Engineering, *Editor Springer, New York*, 1988.

[3] C. Pfistner, R. Weber, S. Merazzi, and R. Gruber, Thermal Beam Distortions in End-Pumped Nd:YAG, Nd:YLF Rods, *IEEE J. Quant. Electron., Q.E.30, pp. 1605-1615*, 1994.

[4] Scaling CW Diode-End-Pumped Nd:YAG Lasers to High Average Powers, IEEE J. Quant. Electron., QE 28, april 1992.

[5] C.R.C Handbook of Laser Science and Technology, Optical Material: Part 2, vol. IV, pp. 15-20 e 319-343, (1988).